CHEMISTRY
A EUROPEAN JOURNAL

DOI: 10.1002/chem.200500501

Unique Nanoscale Morphologies Underpinning Organic Gel-Phase Materials

Andrew R. Hirst,[a] David K. Smith,*[a] and John P. Harrington[b]

Abstract: This study investigates the self-assembly of simple aliphatic diamines with a dendritic peptide. By controlling the molar ratio of this two-component system, new nanoscale morphologies were generated. In the presence of relatively long aliphatic chains (C10, C12) a transition from nanoscale fibres to platelets was observed on changing the molar ratio, whereas, for shorter spacer chains (e.g., C9 and C8), interesting and unique morphological changes were observed by low voltage field emission gun scanning electron microscopy (SEM), with "nanosquares" or nanoscale "rosette" structures being formed. Remarkably, these discrete nanoscale structures were able to form sample-spanning networks capable of supporting a gel-phase material; whereas, most gels are usually based on fibrillar assemblies. In addition to SEM, the gels were characterised by using thermal measurements and circular dichroism spectroscopy. The length of the diamine spacer and the molar ratio of components controlled the self-assembly process by modifying the spatial organisation of the dendritic head groups at the molecular level, which is transcribed into the aspect ratio of the self-assembled state at the microscopic level. Ultimately, this led to diamine-induced control of the macroscopic material's behaviour. When present in excess, the diamine controlled the observed nanoscale morphology as a consequence of undergoing a dendritically controlled nanocrystallisation process to form a network, an unusual and significant result.

Keywords: crystal growth · dendrimers · gels · nanostructures · self-assembly

Introduction

One of the most fascinating aspects of the emergent field of nanochemistry is the ability of self-assembly methods[1] to generate a variety of different morphologies with structural definition on the nanometre scale. The properties of a self-assembled material depend both on the nature of its molecular constituents and the precise spatial positioning of the functional groups. Indeed, in this way, the structural framework of a molecular "building block" can be considered to be programmed with molecular information (e.g., chirality, hydrogen-bonding capacity, steric demands, electrostatic properties, hydrophilic/hydrophobic character and metal-ion binding capability) which enables it to hierarchically self-assemble into a target nanostructure. For example, it has long been recognised that dilute solutions of surfactant molecules can assemble reversibly into different spatially organised nanoscale structures (e.g., cubic, hexagonal or lamellar), depending on surfactant geometry, concentration, co-surfactant or salinity, with sphere-to-rod transitions (and vice versa) of micellar self-assembled states being reported for a range of surfactant-derived molecular assemblies.[2]

Supramolecular gel-phase materials based on low molecular weight "building blocks" (gelators) are particularly interesting nanostructured materials in which the information stored in the molecular species controls the so-called "bottom-up" fabrication of nanoscale architectures.[3] The vast majority of one- and two-component[4] low molecular weight gels consist of three-dimensional networks in which self-assembled "one-dimensional" fibres are capable of immobilising large volumes of organic solvents as a consequence of capillary forces and surface tension. Surprisingly, however, little attention has focused on investigating different types of morphology (i.e., nonfibrous) that can underpin gel-phase materials. Lamellar,[5] vesicle[6] and platelet[7] morphologies have been reported in a limited number of cases, but there is little predictive understanding of the formation of these types of morphology.

[a] Dr. A. R. Hirst, Dr. D. K. Smith
Department of Chemistry, University of York
Heslington, York, YO10 5DD (UK)
Fax: (+44) 1904-432-516
E-mail: dks3@york.ac.uk

[b] J. P. Harrington
Leeds Electron Microscopy and Spectroscopy (LEMAS) Centre
Institute for Materials Research, University of Leeds
Leeds, LS2 9JT (UK)

Recently, we have reported detailed investigations of a two-component dendritic gelation system, which exhibits high levels of structural tunability.[8] This system utilises an acid–base hydrogen-bond interaction (with possible proton transfer) between dendritic L-lysine building blocks and an aliphatic diamine, which yields a gelator complex (see Figure 1). We have shown that this gelator complex hierarchically self-assembles to form fibrous gel-phase materials. Self-assembly occurs as a consequence of intermolecular dendron–dendron hydrogen-bond interactions. Interestingly, we observed that varying the ratio of the two-components (with $n=12$) offered a unique method for achieving morphological tunability.[9] We found that increasing the amount of C12 diamine relative to the dendritic branch changed the propensity of this system to induce macroscopic gelation, and ultimately gave rise to a new morphology in which micrometre-sized platelets were observed.

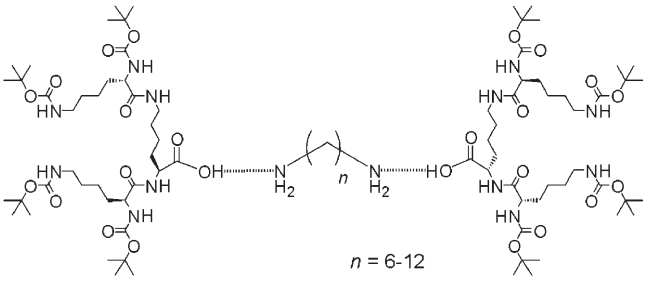

Figure 1. Two-component dendritic gelation system (G2···C*n*···G2) previously reported by us.[8,9]

We therefore decided to develop an understanding of this unique morphological transition, and determine whether any other new nanoscale morphologies could be generated by using this simple approach. As such, this paper focuses on understanding the mode of self-assembly by using different molar ratios of dendron/diamine, and extends the understanding of ways in which different nanostructured morphologies can underpin gelation. This simple molar-ratio tunability is not possible for one-component gelators and is a unique feature of two-component gelation systems. We report that when the diaminoalkane is present in excess, the dendritic component effectively controls the "crystallisation/solubilisation" of the diaminoalkane in order to yield regular, discrete nanostructured architectures. Furthermore, the resultant nanostructures still form extended three-dimensional networks that underpin macroscopic gelation.

Results and Discussion

Synthesis of gelators: The second generation L-lysine-based dendritic branches (dendrons)[10] were synthesised in optically pure form and in high yields, by using a solution-phase approach previously reported by us,[11] with column chromatography being employed to isolate the purified material. The aliphatic diamines were purchased from standard chemical suppliers.

Characterisation of the gel-phase materials constructed by using different molar ratios

Thermal behaviour: From the results presented in our previous paper,[9] it was clear that when using diaminododecane, the dendron/diamine molar ratio directly controlled the nanoscale morphology. Indeed, incremental additions of diaminododecane to the gelation system induced a morphological transition in the self-assembled state, ultimately changing from bundles of fibres that constitute a highly developed entangled network to a system composed of micron-sized platelets (Figure 2).

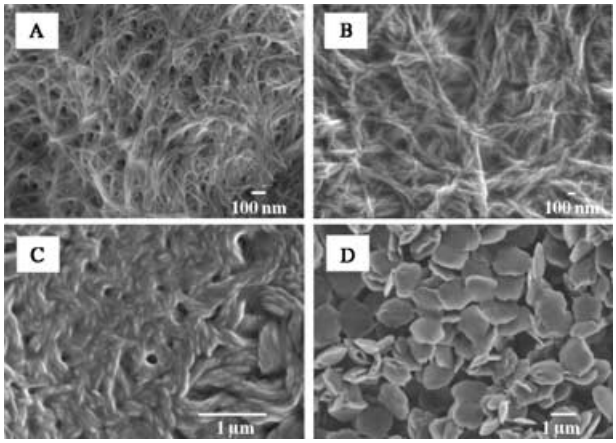

Figure 2. Effect of stoichiometric ratio (dendron/diamine) on gel morphology as imaged by SEM.[9] A) 2:1, [dendron] = 9 mM, [C12] = 4.5 mM. B) 1:1, [dendron] = 9 mM, [C12] = 9 mM. C) 1:2.7, [dendron] = 9 mM, [C12] = 24.3 mM. D) 1:4.5, [dendron] = 9 mM, [C12] = 40.5 mM.

In order to assess the behaviour of gels based on different dendron/diamine molar ratios in more detail than our previous study, the transition from an immobile to a mobile self-assembled state was determined by using tube-inversion experiments across a wide range of molar ratios, and also by using other diamines in addition to diaminododecane (C12), namely diaminodecane (C10), diaminononane (C9) and diaminooctane (C8). This method served to define a mobile-gel transition temperature (i.e., a gel "boundary") and is described in detail in the Experimental Section (the method is highly reproducible and the estimated error is ± 1 °C).[12] For the purpose of this discussion, the gel "boundary" is analogous to the thermally reversible gel–sol transition temperature (T_{gel}). All the gels reported here were optically clear, apart from some systems containing relatively large excesses of diamine (e.g., dendron/C12 ratio of 1:4.5 and dendron/C8 ratio greater than 1:1.7). In these cases, the aggregate state could be observed by the naked eye (i.e., the materials became cloudy). Additionally, when a large excess of diamine was present, it was sometimes difficult to ensure complete solubilisation of the diamine by the dendron. Under certain conditions, unsolubilised diamine was observed to remain in the sample tubes after the heat–cool

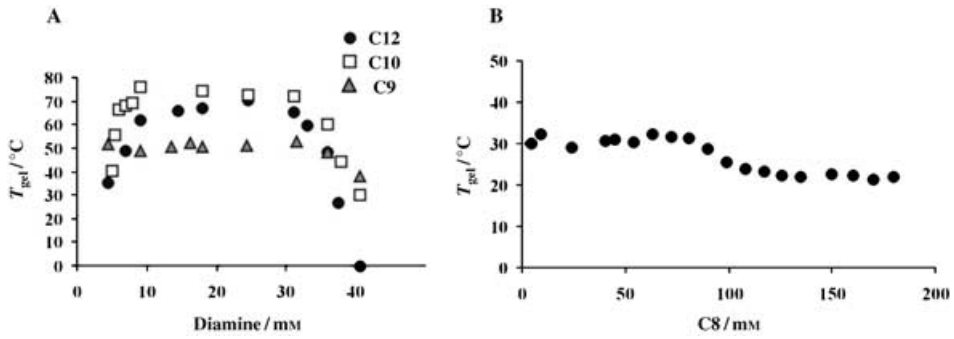

Figure 3. Effect of stoichiometric ratio (dendron/diamine) on the gel–sol transition temperature (T_{gel}). For each measurement $[dendron]_{total} = 9$ mM and solvent = toluene. A) Effect of increasing concentrations of C9, C10 and C12 aliphatic diamines on T_{gel}. B) Effect of increasing concentration of C8 aliphatic diamine on T_{gel}.

cycle. This clearly indicated that only a finite amount of diamine can be solubilised by the dendron. Figure 3 illustrates the effect of molar ratio on the thermal properties of the gel as determined by T_{gel} measurements ([dendron] remains constant at 9 mM for each measurement). The data presented in this figure only relate to those systems in which complete diamine solubilisation could be achieved.

Interestingly, the gels based on C10 and C12 spacer units exhibited similar thermal behaviours. Incremental addition of diamine to the 2:1 dendron/diamine system (i.e., [dendron] = 9 mM, [diamine] = 4.5 mM) increased the T_{gel} value until a maximum was reached at ≈1:1 dendron/diamine ratio, and at this point T_{gel} became independent of the increasing molar ratio. Increasing the amount of diamine further (i.e., beyond ≈1:3.4 dendron/diamine) resulted in an incremental decrease in the thermal stability of the material. At a molar ratio of 1:4.5 (dendron/diamine), the C12-based system was in the "sol" state at ambient temperatures, whereas the C10-based system was a gel with a T_{gel} value of 29 °C.

In comparison with the C12- and C10-based gels described above, the C9 system had a T_{gel} value which was effectively independent of the dendron/diamine molar ratio until a ratio of 1:3.4 (dendron/diamine) was attained. Beyond this point, as the amount of C9 spacer chain was increased further, a decrease in T_{gel} was once again observed, however, this was a relatively minor effect. Indeed, even at a dendron/diamine molar ratio of 1:4.5, macroscopic gelation was still observed with a T_{gel} value of 34 °C, thus exhibiting greater thermal stability than the gels based on C10 or C12 spacers. Therefore, the C9-based gelation system appears to be less thermally responsive to excess diamine than the C10 and C12 systems.

The C8-based gelation system was also studied as a function of molar ratio over an extended concentration range (Figure 2B). Surprisingly, the C8 system exhibited T_{gel} values which were almost independent of molar ratio across the entire extended range studied. Indeed, increasing the amount of C8 diamine from a molar ratio (dendron/diamine) of 2:1 to 1:20 only reduced the thermal stability of the gel from 30 to 22 °C, a change of just 8 °C. In this case, the large excess of diamine therefore appeared to have minimal effect on the macroscopic thermal behaviour of the gel.

These observations may indicate that when employing a C12 or C10 aliphatic diamine, changing the molar ratio modulates the crucial dendron–dendron intermolecular hydrogen-bond interactions.[8] Conversely, when using the C9 or C8 aliphatic diamines, the molar ratio appears to exert less control over these molecular recognition events. This will be discussed in more detail in the following sections.

Morphological behaviour: Molecular self-assembly at the nano- and microlevels was observed by using field emission gun scanning electron microscopy (SEM), a useful comparative visual technique for assessing the impact of the dendron/diamine molar ratio on the mode of self-assembly. This method shed further light on the differences observed in thermal behaviour for the different gels and also led to the visualisation of a wide range of interesting nanoscale morphologies, which, importantly, could be correlated with the macroscopic behaviour of the gel described in the preceding section.

Figure 2A–D shows a series of SEM images[9] of the organogels in which the amount of the C12 aliphatic diamine was incrementally increased. The same concentration of dendron was employed in each case. Clearly, the morphology of the self-assembled state was directly controlled by the amount of C12 diamine present. When the dendron/diamine molar ratio was 2:1 (Figure 2A), thin (ca. 20 nm) fibres were observed, which self-assemble to form bundles of fibres that constitute a high-density entangled network. These regular high aspect-ratio fibres are typical of gel-phase materials and are indicative of unidirectional stacking driven by amide–amide hydrogen bonding. Incrementally increasing the amount of C12 diamine to give a 1:1 dendron/diamine molar ratio modified the nanostructure underpinning gelation. In this case, a network composed of entwined/twisted fibres was observed (Figure 2B). It is important to note that the subtle change in aggregate morphology was reflected by an increase in thermal stability of the gel (dendron/C12 molar ratio = 2:1, T_{gel} = 37 °C; dendron/C12 molar ratio = 1:1, T_{gel} = 62 °C). Increasing the amount of C12 diamine further to give a dendron/diamine molar ratio of 1:2.7 induced a morphological transition to a "rope-like" morphology (Figure 2C). In this case, the morphological transition was not reflected by a further macroscopic change in T_{gel}. Finally, using a dendron/diamine molar ratio of 1:4.5 produced a profound change in the aggregate morphology (Figure 2D). Flattened platelets with diameters of ≈1 μm were observed

throughout the sample. This morphological transition was associated with a major decrease in the observed T_{gel} value. Indeed, the system was no longer a gel at ambient temperature.

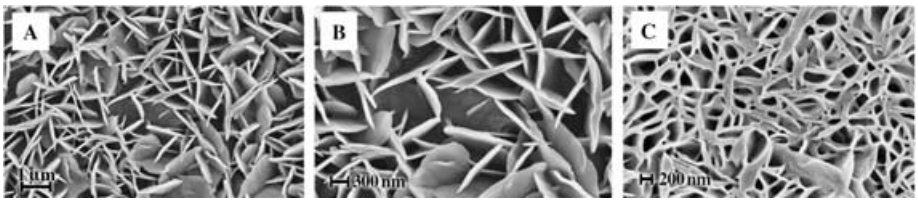

Figure 4. Effect of stoichiometric ratio (dendron/C10 diamine) on gel morphology as imaged by SEM. A) 1:4.5, [dendron] = 9 mM, [C10] = 40.5 mM (total image). B) 1:4.5, [dendron] = 9 mM, [C10] = 40.5 mM (zoomed in). C) 1:5, [dendron] = 9 mM, [C10] = 45 mM.

It is informative to compare this morphological transition with the thermal behaviour of the gel. Initially, increasing the amount of diamine appears to promote the formation of more thermally stable gels. We therefore infer that the initial increase in the amount of diamine promotes the formation of dendron–dendron hydrogen bonds within the fibres, presumably by alleviating steric crowding effects between the dendritic head groups. However, when the amount of diamine is increased further, it is likely that the relatively small amounts of dendron become too spatially isolated to effectively stabilise anisotropic fibrous self-assembly. We postulate that under these excess diamine conditions, the dendron acts simply to ensure the diamine is compatible with the apolar solvent. The dendron and diamine interact with one another through acid–base interactions, but the dendrons become spatially isolated and unable to intermolecularly hydrogen bond to one another within fibres. This leads to the generation of a platelet morphology and the observed decrease in T_{gel} value; indeed, gels only resulted on cooling the samples.

We propose that the dendron controls the aggregation of the diamine, which undergoes a controlled "crystallisation/solubilisation" process, with a layer of dendron adsorbed onto its surface. In other words, once a sufficient excess of the diamine is present, it aggregates in a controlled manner (due to the presence of small amounts of dendron). It is worth noting that the controlled crystallisation of organic species (such as the diaminoalkane in this case) is rare.[13] There are, however, a large number of examples of additives directing crystallisation of a variety of inorganic substrates, indeed this is one of the most exciting frontiers of nanochemistry.[14] Interestingly, in a recent report, alkylamines were used to modify the growth of silica, with the fabrication of a network of lotus-leaf-like flakes with diameters of $\approx 3\,\mu m$ and thicknesses of ≈ 200 nm, similar to the structures shown in Figure 2D.[15] Furthermore, it was recently reported that $NbSe_2$ could either assemble into two-dimensional platelets or a fibrous morphology, dependent primarily on the ratio of surfactant to inorganic intermediate after washing and before heating.[16]

With a model for the formation of the platelet morphology in hand, we went on to investigate the effect of changing the spacer chain. The gel based on a dendron/C10 molar ratio of 1:4.5 was imaged by using SEM (Figure 4A,B). The aggregate morphology was similar to the system based on the C12 diamine, with platelets having dimensions of $\approx 1\,\mu m$ being formed. However, on comparison with the C12 system, the platelets appeared to be more effectively fused together forming a continuous network. Interestingly, this system still formed a gel-phase material at ambient temperature ($T_{gel} = 29\,^{\circ}C$), indicating that the three-dimensional network of fused platelets underpins macroscopic gelation. This extended network became even more evident on increasing the molar ratio to 1:5, at which point an irregular honeycomb microstructure was observed (Figure 4C). There are very few examples in the literature in which gel-phase materials have been clearly demonstrated to be constructed from platelet networks,[7] and this makes this irregular honeycomb morphology of particular interest. Interestingly, the gelation of paraffin waxes[7a] gives rise to a "stacked platelet" morphology, and it was argued that the hydrocarbon gelators crystallise into thin microplatelets—with the crystals growing at approximately equal rates along two Cartesian axes, and at a much slower rate along the third—analogous to our system.

To further investigate the effect of the spacer chain on this type of morphological transition, the C9-based system was also studied by using SEM. As reported previously,[8b] the 2:1 (dendron/diamine) organogel was composed of fibres with widths of approximately 30–40 nm and a polydispersity of lengths (Figure 5A). Initially, increasing the amount of C9 aliphatic chain had only a small effect on the observed aggregate morphology (Figure 5A–C), in contrast to the system based on the C12 diamine. Interestingly, this is in agreement with the T_{gel} values reported above, which

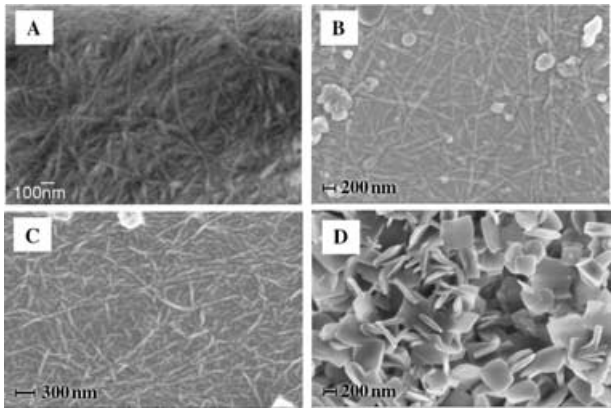

Figure 5. Effect of stoichiometric ratio (dendrimer/C9 diamine) on gel morphology as imaged by SEM. A) 2:1, [dendron] = 9 mM, [C9] = 4.5 mM. B) 1:1, [dendron] = 9 mM, [C9] = 9 mM. C) 1:2.7 [dendron] = 9 mM, [C9] = 24.3 mM. D) 1:4.5, [dendron] = 9 mM, [C9] = 40.5 mM.

were effectively independent of molar ratio. This observation is potentially a consequence of the different steric demands when forming a fibrillar assembly using the smaller spacer chain.

Intriguingly, at a molar ratio of 1:4.5, a difference in the aggregate morphology was eventually observed (Figure 5D) corresponding to the slight decrease in T_{gel} value. In this case, nanosized flattened square-shaped aggregates were observed, with widths of approximately 200–400 nm. These structures are considerably smaller than the micron-sized platelets observed with the C10 and C12 diamines, and importantly, have a different shape. To the best of our knowledge, these flat nanosquares constitute a unique nanoscale morphology. Furthermore, this system was a self-supporting gel suggesting that these nanosquares form a sample-spanning network, capable of underpinning macroscopic gelation. Figure 5D supports this hypothesis: it can be seen that some of the square-shaped aggregates are "fused" together. Once again, we postulate that the dendron stabilises the surface of growing diamine nanocrystals. In this case, however, the "crystallisation" preference of the C9 diamine gives rise to this unique morphology, and in this way is expressed on the nanoscale. It is noteworthy that nanocrystalline structuring of organic compounds in this way is extremely difficult, indeed the pursuit of organic nanocrystals is one of the key frontier research areas in pharmaceutical formulation of organic drugs.[17]

Finally, the supramolecular gel based on the C8 aliphatic diamine was investigated. As shown above, the macroscopic thermal stability of the gel was effectively independent of the excess amount of diamine. Indeed, gel-phase materials were still formed, even with a large excess of diamine present. It proved impossible to image the gel-phase materials with relatively low amounts of the C8 diamine ($<$1:4.5). Interestingly, at a dendron/C8 molar ratio of 1:4.5, a mixture of platelet aggregates ($\approx$1.5 μm) and rosette-like structures was imaged (Figure 6A). Increasing the amount of C8 diamine to give a dendron/C8 molar ratio of 1:5 (Figure 6B) yielded a microstructure composed entirely of rosette-like structures. Each individual rosette had a width of approximately 1 μm, being composed of smaller individual fused nanoscale platelets. Rosette, or flower-like morphologies are known to arise from controlled crystallisation processes.[18] Once again, we propose that dendritically controlled surface stabilisation of the aliphatic C8 diamine gives rise to this nanocrystalline morphology. It is important to reiterate that our rosette morphology is not a "crystalline" solid as such, rather it underpins macroscopic gelation, thus indicating that, unusually, this nonfibrous morphology constitutes a gel-phase material underpinned by a sample-spanning network.

Using the C8 spacer, however, an intriguing second morphological transition was also observed. At a dendron/C8 molar ratio of 1:6, a total morphological transition from the rosette microstructure to a "sponge-like" morphology was observed (Figure 6C), still macroscopically a gel. Finally, at a dendron/C8 diamine molar ratio of 1:10 a "film-like" morphology was imaged in which all fine detail was lost (Figure 6D). Interestingly, this morphology still underpins macroscopic gelation, although it was noted that this material now exhibited an enhanced extensional viscosity (i.e., the material could be stretched out of the sample tube). This intriguing behaviour, which can only be accessed by using the two-component system with a shorter C8 spacer chain, will be the subject of further investigations. It is remarkable that through all these morphology changes, the T_{gel} value remains almost invariant, an observation that indicates there can be only subtle differences between the hydrogen-bond network connectivities associated with the different morphologies.

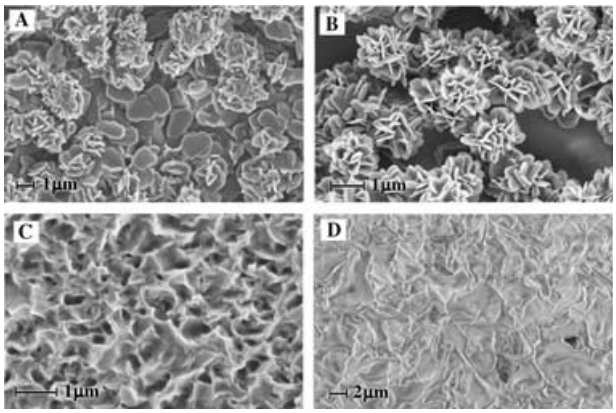

Figure 6. Effect of stoichiometric ratio (dendrimer/C8 diamine) on gel morphology as imaged by SEM. A) 1:4.5, [dendron] = 9 mM, [C8] = 40.5 mM. B) 1:5, [dendron] = 9 mM, [C8] = 45 mM. C) 1:6, [dendron] = 9 mM, [C8] = 54 mM. D) 1:10, [dendron] = 9 mM, [C8] = 90 mM.

Circular dichroism (CD) studies: CD spectra[19] appear when the chromophoric moieties of chiral molecules are organised into an appropriate helical orientation.[20] Our investigations were performed in the dilute state (i.e., below the gelation threshold) to facilitate sample handling and using cyclohexane as the aprotic solvent. CD peaks with λ_{max} values at $\approx$222 nm were observed, ascribable to supramolecular chiral organisation of the amide carbonyl group of the dendritic peptides (Figure 7A). This suggests that a chirally ordered (helical) arrangement is present in the self-assembled state, even below the gelation threshold. In each case, the CD signal had a negative sign, indicating that the bias of the supramolecular chirality (or helicity) had the same directionality in each assembly.

The effects on helicity of changing both the aliphatic spacer chain and the molar ratio of the two components are shown in Figure 7B–D. Interestingly, both the length of the spacer unit and the molar ratio of the components modulated the magnitude of the CD band, and consequently, the level of nanoscale chiral organisation present in the self-assembled state.

For the C12-based organogels (Figure 7B), initially increasing the amount of C12 relative to the dendron increased the magnitude of the CD signal, and consequently,

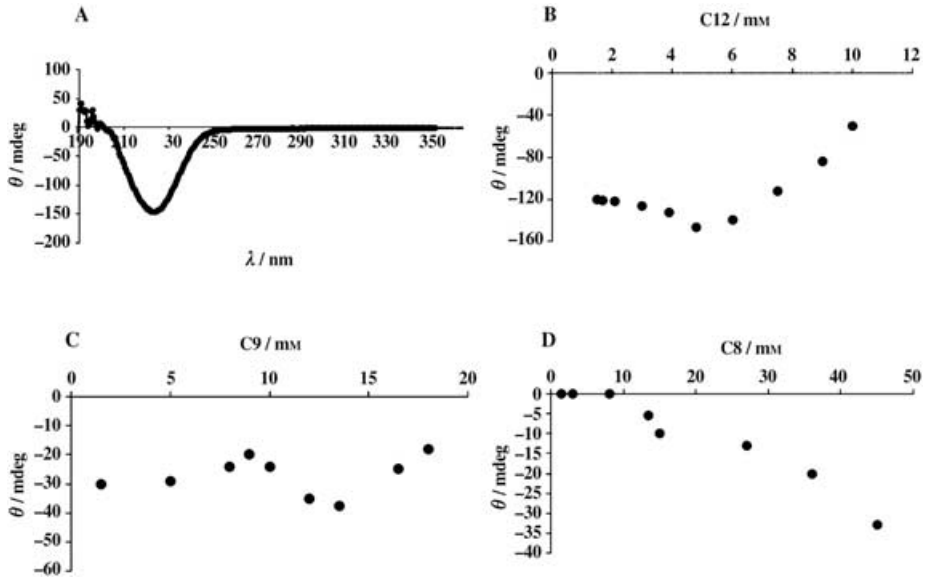

Figure 7. A) Typical CD spectra of self-assembled materials (below the gelation threshold concentration) in cyclohexane at room temperature: [dendron] = 3 mM, [C12] = 4.8 mM. B–D) Effect of incremental addition of diamine on ellipticity: [dendron] = 3 mM, B = C12, C = C9, D = C8.

the degree of nanoscale chiral ordering in the self-assembled state can be considered to be enhanced. An optimum chiral organisation of the dendritic head groups was attained at a dendron/diamine molar ratio of 1:1.6. Interestingly, this can be related to the formation of entwined/twisted morphologies that also underpinned the onset of maximum T_{gel} values (Figure 2B). Beyond this optimum value, incremental additions of C12 diamine resulted in a gradual loss of chiral organisation. However, even at a dendron/C12 molar ratio of 1:3.3 the self-assembled state still exhibited a degree of helicity. It is interesting to speculate whether the dendritic head groups at the surface of the platelets observed in SEM (dendron/diamine, 1:4.5) would be chirally ordered. Unfortunately, is was impossible to determine this due to the opacity of the sample.

It appears that for the C12-based gel, an optimum exists between diamine content and chiral organisation. We argue that this is related to the effective packing of the dendritic head groups and the need to solubilise an increasing amount of diamine. On the one hand, initially increasing the diamine content above a dendron/diamine molar ratio of 2:1 promotes chiral organisation as this can alleviate unfavourable steric repulsive effects between dendritic head groups and enable efficient dendron–dendron hydrogen bonding. However, on the other hand, increasing the diamine content beyond the optimum value effectively forces the dendritic head groups further apart as the volume of diamine that must be solubilised increases. In this way, the molecular recognition process between dendritic head groups becomes weaker. It is clear that for this system, the nanoscopic chiral organisation can be directly correlated to the thermal properties of the gel (i.e., T_{gel} values), indicating that effective dendron organisation is the essential feature which underpins the formation of a gel-phase extended network.

Interestingly, the chiral organisation of C9-based self-assemblies was effectively invariant to the amount of spacer unit in the system. This can, once again, be correlated with the thermal properties of the material, which showed a similar invariance, and indicates that hydrogen bonds between chirally organised dendrons are the essential prerequisite for the formation of an extended network. Furthermore, we can infer from this data that the dendritic head groups formed at the surface of the nanosquare assemblies are chirally ordered, as a CD signal is still observed for the system with a molar ratio of 1:4.5 (dendron/diamine). This is a key result, as it indicates that we are forming discrete chiral nanoscale objects by using a self-assembly (bottom-up) fabrication approach.

For the C8-based organogels, an intriguing transition from an achiral to a chiral self-assembled state was observed as the amount of C8 diamine was incrementally increased. At 2:1 molar ratios, where it was not possible to image a morphology by SEM, there was effectively no nanoscale chiral order. However, with more diamine present, the chiral ordering was enhanced. This indicates that the "film-like" morphology formed in the presence of a large excess of dendron actually has the greatest degree of chiral organisation of the dendritic head groups. It is possible that this may be connected to the interesting macroscopic properties (i.e., enhanced extensional viscosity) of this material, and this possibility is currently under further investigation. However, once again, it is clear that as the spacer chain becomes smaller, the features which control organised self-assembly and the morphological transitions associated with them, change significantly.

Conclusion

It is apparent that changing the molar ratio of the two components in these gel-phase materials controls the morphology of the self-assembled state, making this system of interest for bottom-up nanofabrication of materials with different thermal properties and nanoscale chiral organisation. We propose that at relatively high mole fractions of diamine, the dendron acts to stabilise the surface of organised discrete regions of aliphatic diamine, and a controlled "crystallisation" process beings to dominate the aggregate morphology. Ultimately, in each case, excess diamine causes a dramatic morphological transition from extended fibrous as-

semblies to discrete nanosized objects. Unique, new nanoscale morphologies such as squares and rosettes were observed, which were fascinatingly still capable of forming extended gel-phase networks. This is consistent with the proposal that when excess diamine is present, dendritically controlled "nanocrystallisation" becomes the dominant feature of macroscopic gelation, with the length of the diamine spacer chain controlling the preferred morphology of the observed nanocrystals. Organic nanocrystals are of considerable interest, as they have previously proven very difficult to fabricate. Furthermore, nonfibrillar supramolecular gels are rare. In the future, we aim to exploit gels with different nanostructures and attempt to harness their morphologies to achieve new forms of functional behaviour.

Experimental Section

Materials: The L-lysine-based dendritic branches[10] (dendrons) were synthesised in optically pure form and in high yields by using a solution-phase approach previously reported by us,[11] with column chromatography being employed to isolate the purified material. The aliphatic diamines were purchased from Aldrich (C8, C10, C12) and Lancaster (C9).

Gelation experiments: The experiment was performed by solubilisation of a weighed amount of dendritic gelator in a measured volume of selected pure solvent. The mixture was sonicated at ambient temperature for 30 min before heating and cooling produced a gel. The gel sample was left to stand overnight. Gelation was considered to have occurred when a homogenous "solid-like" material was obtained that exhibited no gravitational flow. The thermally reversible gel–sol transition temperature (T_{gel}) was determined by using a tube-inversion methodology. The gel–sol transition temperature represents the point at which the stress exerted by the gel exceeds its yield strength and a drop of solvent begins to run from the immobilised gel. All samples of gel-phase materials were prepared with a total volume of 1 mL in tubes with a diameter of 10 mm. This ensures that the stress generated by the gel on tube inversion is approximately constant in each case.

Low voltage field emission gun scanning electron microscopy (SEM): Gel samples were applied to standard aluminium SEM stubs and allowed to dry. Prior to examination, the gels were coated with a thin layer (5 nm) of Pd/Pt using an Agar high-resolution sputter coater fitted with a thickness monitor/controller. Scanning electron micrographs were recorded by using a LEO 1530 Gemini FEGSEM instrument operated at 3 keV. The standard SEM images in Figure 3A–D and Figure 5A were obtained by using a Jeol JSM-6330F instrument. Prior to examination, the gels were coated with a thin layer of gold/Pt (60:40). Au/Pt deposition was performed by using a Denton vacuum LLC.

Circular dichroism (CD) measurements: CD spectra were recorded in the ultraviolet region (200–350 nm) by using a JASCO 810 spectrometer and a 1.0 mm quartz cuvette. A sample interval of 1 nm and an averaging time of 3 s were used in all experiments. [Dendritic branch] = 3 mM.

Acknowledgement

This work was supported by the Engineering and Physical Sciences Research Council (EPSRC, EP/C520750/1) in the UK.

[1] a) G. M. Whitesides, B. Grzybowski, *Science* **2002**, *295*, 2418–2421; b) I. W. Hamley, *Angew. Chem.* **2003**, *115*, 1730–1752; *Angew. Chem. Int. Ed.* **2003**, *42*, 1692–1712; c) J. J. L. M. Cornelissen, A. E. Rowan, R. J. M. Nolte, N. A. J. M. Sommerdijk, *Chem. Rev.* **2001**, *101*, 4039–4070; d) G. M. Whitesides, M. Boncheva, *Proc. Natl. Acad. Sci. USA* **2002**, *99*, 4769–4774; e) D. K. Smith, A. R. Hirst, C. S. Love, J. G. Hardy, S. V. Brignell, B. Huang, *Prog. Polym. Sci.* **2005**, *30*, 220–293.

[2] B. Jönsson, B. Lindman, K. Holmberg, B. Kronberg, *Surfactants and Polymers in Aqueous Solution*, Wiley, Chichester, UK, **1998**.

[3] a) P. Terech, R. G. Weiss, *Chem. Rev.* **1997**, *97*, 3133–3159; b) O. Gronwald, E. Snip, S. Shinkai, *Curr. Opin. Colloid Interface Sci.* **2002**, *7*, 148–156; c) J. H. van Esch, B. L. Feringa, *Angew. Chem.* **2000**, *112*, 2351–2354; *Angew. Chem. Int. Ed.* **2000**, *39*, 2263–2266; d) R. Oda, I. Huc, S. J. Candau, *Angew. Chem.* **1998**, *110*, 2835–2838; *Angew. Chem. Int. Ed.* **1998**, *37*, 2689–2691; e) D. J. Abdallah, R. G. Weiss, *Adv. Mater.* **2000**, *12*, 1237–1247; f) T. Shimizu, *Polym. J.* **2003**, *35*, 1–22.

[4] For a review of two-component gels, see: A. R. Hirst, D. K. Smith, *Chem. Eur. J.* **2005**, *11*, 5496–5508.

[5] a) H. Kobayashi, M. Amaike, J. H. Jung, A. Friggeri, S. Shinkai, D. N. Reinhoudt, *Chem. Commun.* **2001**, 1038–1039; b) M. Gradzielski, *J. Phys. Condens. Matter* **2003**, *15*, R655–R697; c) F. M. Menger, A. V. Peresypkin, *J. Am. Chem. Soc.* **2003**, *125*, 5340–5345; d) M. Dukh, D. Saman, J. Kroulik, I. Cerny, V. Pouzar, V. Kral, P. Drasar, *Tetrahedron* **2003**, *59*, 4069–4076.

[6] a) J. H. Jung, S. Shinkai, T. Shimizu, *Chem. Eur. J.* **2002**, *8*, 2684–2690; b) T. Sato, M. Seko, R. Takasawa, I. Yoshikawa, K. Araki, *J. Mater. Chem.* **2001**, *11*, 3018–3022; c) C. Kim, K. T. Kim, Y. Chang, H. H. Song, T.-Y. Cho, H.-J. Jeon, *J. Am. Chem. Soc.* **2001**, *123*, 5586–5587; d) S. M. Park, Y. S. Lee, B. H. Kim, *Chem. Commun.* **2003**, 2912–2913.

[7] a) D. J. Abdallah, S. A. Sirchio, R. G. Weiss, *Langmuir* **2000**, *16*, 7558–7561; b) H. S. Ashbaugh, A. Radulescu, R. K. Prud'homme, D. Schwahn, D. Richter, L. J. Fetters, *Macromolecules* **2002**, *35*, 7044–7055; c) R. Schmidt, F. B. Adam, M. Michel, M. Schmutz, G. Decher, P. J. Mésini, *Tetrahedron Lett.* **2003**, *44*, 3171–3174.

[8] a) K. S. Partridge, D. K. Smith, G. M. Dykes, P. T. McGrail, *Chem. Commun.* **2001**, 319–320; b) A. R. Hirst, D. K. Smith, M. C. Feiters, H. P. M. Geurts, *Langmuir* **2004**, *20*, 7070–7077; c) A. R. Hirst, D. K. Smith, *Org. Biomol. Chem.* **2004**, *2*, 2965–2971; d) A. R. Hirst, D. K. Smith, *Langmuir* **2004**, *20*, 10851–10857; e) A. R. Hirst, D. K. Smith, M. C. Feiters, H. P. M. Geurts, *Chem. Eur. J.* **2004**, *10*, 5901–5910.

[9] A. R. Hirst, D. K. Smith, M. C. Feiters, H. P. M. Geurts, A. C. Wright, *J. Am. Chem. Soc.* **2003**, *125*, 9010–9011.

[10] For the original report of dendrimers based on L-lysine, see: a) R. G. Denkewalter, J. Kolc, W. J. Lukasavage, (Allied Corp) US 4289872, **1981**; [*Chem. Abstr.* **1985**, *102*, 79324q]. A number of other gel-phase materials based on L-lysine have been reported, see for example: b) K. Hanabusa, H. Nakayama, M. Kimura, H. Shirai, *Chem. Lett.* **2000**, 1070–1071; c) M. Suzuki, M. Yumoto, H. Kimura, H. Shirai, K. Hanabusa, *Helv. Chim. Acta* **2004**, *87*, 1–10, and references therein.

[11] a) G. M. Dykes, L. J. Brierley, D. K. Smith, P. T. McGrail, G. J. Seeley, *Chem. Eur. J.* **2001**, *7*, 4730–4739; b) M. Driffield, D. M. Goodall, D. K. Smith, *Org. Biomol. Chem.* **2003**, *1*, 2612–2620.

[12] a) C. Chaibundit, M. Shao-Min, F. Heatley, C. Booth, *Langmuir* **2000**, *16*, 9645–9652; b) A. Kelarakis, Z. Yang, E. Pousia, S. K. Nixon, C. Price, C. Booth, I. W. Hamley, V. Castelletto, J. Fundin, *Langmuir* **2001**, *17*, 8085–8091.

[13] a) H. Fu, D. Xiao, J. Yao, G. Yang, *Angew. Chem.* **2003**, *115*, 2989–2992; *Angew. Chem. Int. Ed.* **2003**, *42*, 2883–2886; b) F. Bertorelle, D. Lavabre, S. Frey-Forgues, *J. Am. Chem. Soc.* **2003**, *125*, 6244–6253.

[14] For reviews of this approach to nanoscale fabrication, see: a) S. Mann, *Angew. Chem.* **2000**, *112*, 3532–3548; *Angew. Chem. Int. Ed.* **2000**, *39*, 3393–3406; b) H. Colfen, S. Mann, *Angew. Chem.* **2003**, *115*, 2452–2468; *Angew. Chem. Int. Ed.* **2003**, *42*, 2350–2365; c) M. A. López-Quintela, *Curr. Opin. Colloid Interface Sci.* **2003**, *8*, 137–144. For an important theoretical view, see: d) R. L. Whetten, W. M. Gelbart, *J. Phys. Chem.* **1994**, *98*, 3544–3549.

[15] W. Shan, B. Wang, Y. Zhang, Y. Tang, *Chem. Commun.* **2005**, 1877–1879.
[16] P. Sekar, E. C. Greyson, J. E. Barton, T. W. Odom, *J. Am. Chem. Soc.* **2005**, *127*, 2054–2055.
[17] For a review, see: R. H. Muller, C. M. Keck, *J. Biotechnol.* **2004**, *113*, 151–170.
[18] For selected recent examples, see: a) J. Yang, L. Qi, D. Zhang, J. Ma, H. Cheng, *Cryst. Growth Des.* **2004**, *4*, 1371–1375, and references therein; b) J. Zhang, J. Lin, *J. Cryst. Growth* **2004**, *271*, 207–215.
[19] For an overview of CD spectroscopy, see: N. Berova, K. Nakanishi, R. W. Woody, *Circular Dichroism: Principles and Applications*, 2nd ed., Wiley–VCH, Weinheim, **1994**.
[20] For selected examples, see: a) K. Hanabusa, K. Okui, K. Karaki, M. Kimura, H. Shirai, *J. Colloid Interface Sci.* **1997**, *195*, 86–93; b) E. Snip, S. Shinkai, D. N. Reinhoudt, *Tetrahedron Lett.* **2001**, *42*, 2153–2156; c) H. Ihara, M. Takafuji, T. Sakurai, M. Katsumoto, N. Ushijima, T. Shirosaki, H. Hachisako, *Org. Biomol. Chem.* **2003**, *1*, 3004–3006; d) K. Hanabusa, Y. Maesaka, M. Kimura, H. Shirai, *Tetrahedron Lett.* **1999**, *40*, 2385–2388; e) H. Goto, H. Q. Zhang, E. Yashima, *J. Am. Chem. Soc.* **2003**, *125*, 2516–2523; f) J. J. van Gorp, J. A. J. M. Vekemans, E. W. Meijer, *J. Am. Chem. Soc.* **2002**, *124*, 14759–14769.

Received: May 4, 2005
Published online: August 10, 2005

